Improving color homogeneity measure in superpixel segmentation assessment

Isabela B. Barcelos*, Felipe de C. Belém†, Leonardo de M. João†, Alexandre X. Falcão† and Silvio J. F. Guimarães*
*Pontifical Catholic University of Minas Gerais, Belo Horizonte, Brazil
Email: {isabela_borlido@hotmail.com, sjamil@pucminas.br}
†University of Campinas, Campinas, Brazil
Email: {felipe.belem, leonardo.joao, afalcao}@ic.unicamp.br

***Abstract*—The quality of a superpixel segmentation may consider accuracy in delineation, shape compactness, and color homogeneity. Among several existing measures, Explained Variation (EV) and Intra-cluster Variation (IV) seem to be the only ones focusing on color homogeneity. However, EV ignores color differences inside superpixels while IV reduces penalization by averaging those differences. This work proposes a superpixel color descriptor to measure color homogeneity when comparing superpixel algorithms. Our *RGB-cube Bucket Descriptor* (RBD) is a compact representation of the most relevant colors in each superpixel. Color homogeneity is measured based on differences between pixel color and its closest color in RBD and the color differences inside RBD. We call it *Similarity between Image and Reconstruction from Superpixels* (SIRS) since, substituting each pixel color by its closest color in RBD, one obtains an image reconstruction. A high-quality superpixel segmentation should then present a reconstruction similar to the original image. Experiments on three datasets show that SIRS can better distinguish segmentation algorithms according to color homogeneity than EV (the most popular measure). The results also show that SIRS is more robust to slight color variations due to luminosity than EV.**

I. Introduction

A common approach for image segmentation is to generate disjoint groups of connected pixels, named *superpixels*, concerning a predetermined criterion (*e.g.*, color similarity). Such procedure has several benefits: (i) workload magnitude reduction (*i.e.*, pixels to superpixels); (ii) high-level semantic information by the superpixels; and (iii) accurate object delineation by its compounding superpixels. Consequently, superpixel segmentation methods have been used in several applications, such as object segmentation [1], semantic segmentation [2], object detection [3], saliency detection [4], and image classification [5].

Several measures have been proposed to assess superpixel segmentation quality accoding to delineation accuracy, shape compactness and color homogeneity [6]. For instance, one may compare superpixel algorithms according to their accuracy in object delineation using measures such as *Boundary Recall* (BR) [7] and *Under-segmentation Error* (UE) [8]. Informally, BR measures the ratio of object boundaries overlapped by superpixel borders. UE estimates the superpixel error for multiple object overlapping. Some of these measures are also highly correlated [6].

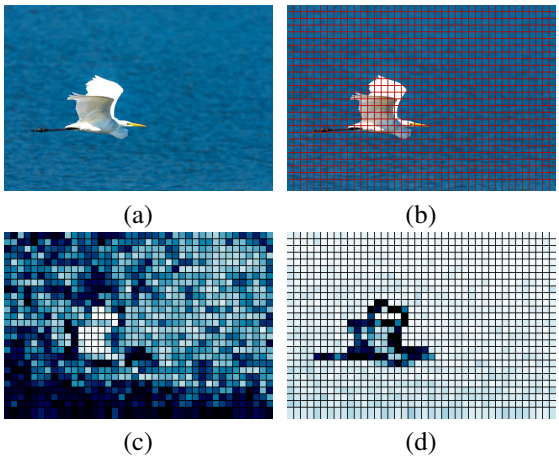

Fig. 1. (a) Original image. Difference between color homogeneity scores for (b) a grid segmentation with 1000 superpixels using (c) EV and (d) our proposal (whiter values indicate higher scores).

Superpixel methods generally aim to generate a controllable number of superpixels composed of connected pixels homogeneous in color. Although the desired properties of superpixels are not a consensus in the literature, inner color similarity usually underlies these methods. Among the proposed measures, *Intra-cluster Variation* (IV) [9] and *Explained Variation* (EV) [10] are the only ones that assess color homogeneity. IV computes the standard deviation of the pixel colors in each superpixel and averages them. It then reduces penalization for superpixels with subtle color variations. However, by not being a normalized measure, IV is not comparable between images nor with other measures [6]. On the other hand, EV ignores color differences inside superpixels. It computes the differences between each superpixel's mean color and the mean color of the image. Despite its popularity [6], [11], EV cannot describe perceptually homogeneous regions in some situations. Figure 1(a) shows an image with slight color variations due to luminosity. EV cannot capture the color homogeneity of a simple grid segmentation.

One could argue that a superpixel should be composed of a small set of representative colors that are not very different from each other. Such a set of colors should represent a perceptually homogeneous superpixel. Ideally, such quantity

should be minimal for an acceptable description, being only one when it is monochromatic. In this work, we achieve that goal with a new measure, named *Similarity between Image and Reconstruction from Superpixels* (SIRS), that relies on a suitable color descriptor for superpixels. SIRS computes the differences between the original and reconstructed images from superpixels. The color descriptor, named *RGB-cube Bucket Descriptor* (RBD), creates a small set of the most relevant colors for each superpixel. One obtains an image reconstruction by substituting each pixel color with its closest color in the RBD of the corresponding superpixel.

In summary, RBD exploits the well-behaved RGB space, described by a cube in $\mathbb{R}^3$, and groups colors based on their similarities to the cube's vertices. Then, each group is divided into several subgroups, and the most relevant colors are selected for superpixel description. With the chosen colors, the image is reconstructed by painting each pixel inside the superpixel with the most similar color available. From that, we use a *Mean Exponential Error* (MEE) to express the reconstruction error between the original and the reconstructed images from RBD. Briefly, MEE increases the error impact for complex textures while reducing the influence on perceptually homogeneous ones. Finally, SIRS defines segmentation quality as the Gaussian weighted error of reconstruction using MEE. By doing so, SIRS provides values normalized between zero and one with adequate spread to differentiate between segmentation qualities easily. Experimental results show its ability to properly penalize superpixels containing heterogeneous colors while maintaining high scores for perceptually homogeneous ones. Also, they show that the measure properly expresses discrepancies between different segmentation qualities using three superpixel segmentation methods in three datasets.

This paper is organized as follows. While Section II formally describes preexisting color-based superpixel measures, our proposal is presented in Section III. Experimental results are thoroughly detailed in Section IV. Finally, we draw conclusions and possible future work in the Section V.

II. Color-based Measures

In this section, we review color-based superpixel measures. Let an *image* $\mathcal{I}$ be defined as a pair $(\mathbf{I}, I)$ in which $\mathbf{I} \subset \mathbb{Z}^2$ is the set of *picture elements* (*i.e.*, *pixels*) whose *colors* is a vector mapped by $I(p) \in \mathbb{R}^m$, given $m \in \mathbb{N}^*$. Note that, when $m = 1$, $\mathcal{I}$ is *grayscale* and it is *colored* otherwise. We may compute the ℓ-*norm* of $I(p) = \langle I_1(p), \ldots, I_m(p) \rangle$ of the colors of the pixel p by $\|I(p)\|_\ell = \left(\sum_{j=1}^{m} |I_j(p)|^\ell \right)^{1/\ell}$, given $\ell \in \mathbb{N}^*$. By setting $\ell = 1$ and $\ell = 2$, the ℓ-norm is equivalent to the *Manhattan* and *Euclidean* distances, respectively.

If a set $X \subseteq \mathbf{I}$ of pixels is provided, one may calculate its *mean color* $\mu(X) \in \mathbb{R}^m$ by $\mu(X) = \frac{\sum_{x \in X} I(x)}{|X|}$, where $|X|$ denotes its size. Furthermore, we may *segment* X into $k \in \mathbb{N}^*$ subsets by a function $\mathbf{S}(X, k) \in \mathbb{P}(X) \setminus \emptyset$, being $\mathbb{P}$ the *power set*, resulting in a *partition* (or *grouping*) $\{X_1, \ldots, X_k\}$ such that $\bigcup_{i=1}^{k} X_i = X$, $\bigcap_{i=1}^{k} X_i = \emptyset$, and $k \leq |X|$. We may extend such concepts for describing the *segmentation* $S \in \mathbf{S}(\mathbf{I}, k)$ of an image $\mathcal{I}$, in which every S_i is a *region* or *superpixel*.

Followed by the intuition that uniformity exhibits low color variability towards the mean, the *Intra-cluster Variation* (IV) [9] measures homogeneity of a superpixel S_i by its standard color deviation. Consequently, as shown in Equation (1), the homogeneity of an image $\mathcal{I}$ is defined as the mean color homogeneity of the segmentation S:

$$IV(S) = \frac{1}{|S|} \sum_{S_i \in S} \frac{\sqrt{\sum_{p \in S_i} \|I(p) - \mu(S_i)\|_1^2}}{|S_i|} \tag{1}$$

One major drawback of IV is not presenting normalized values, being not comparable across images and datasets [6]. Moreover, it penalizes all superpixels equally within the computation [11]. That is, the importance of each region, and thus its deviation, is equivalent irrespective of its size. Finally, by definition, the mean color amortizes the color variations within the superpixel, possibly resulting in an inaccurate color when the composing ones are significantly discrepant.

In contrast to IV, the *Explained Variation* [10] defines homogeneity by comparing the variance of the superpixels' mean color $\mu(S_i)$ and the variance of the pixels' color $I(p)$ towards the image's mean color $\mu(\mathbf{I})$, resulting in a normalized measure (Equation 2). This measure is maximum when $|S| = |\mathbf{I}|$ or when $I(p) = \mu(S_i)$ for all $p \in S_i$ and for every $S_i \in S$.

$$EV(S) = \frac{\sum_{S_i \in S} |S_i| \, \|\mu(S_i) - \mu(\mathbf{I})\|_1^2}{\sum_{p \in \mathbf{I}} \|I(p) - \mu(\mathbf{I})\|_1^2} \tag{2}$$

However, similarly to IV, EV considers the superpixels' mean color, which is insufficient for describing perceptually homogeneous textures [10].

III. Proposal

In this work, we assess the quality of the superpixel segmentation by its ability to reconstruct the original image. More formally, let $\mathcal{R} = (\mathbf{I}, R)$ be a *reconstructed image* of $\mathcal{I}$ in which every pixel $p \in \mathbf{I}$ has its reconstructed (or predicted) color $R(p) \in \mathbb{R}^m$. Such reconstruction is ideal when $R \equiv I$. If a segmentation S is provided, the popular approach is to assign $R(p) = \mu(S_i)$ for all $p \in S_i$ and every $S_i \in S$.

However, as previously discussed, reconstructing $\mathcal{I}$ using the mean value of each superpixel in S leads to inaccurate results. Thus, we propose a superpixel color descriptor, named *RGB Bucket Descriptor* (RBD), in which a palette of the most representative colors within the superpixel $S_i \in S$ is constructed (Section III-A). From that, we build the best reconstruction possible given S and evaluate its similarity towards $\mathcal{I}$ using a novel measure named *Similarity between Image and Reconstruction from Superpixels* (SIRS), described in Section III-B.

A. RGB Bucket Descriptor

We argue that the color information of any superpixel can be represented by a minimal set of colors due to its homogeneity property. In order to build the palette of the most relevant colors in each superpixel $S_i \in S$, we exploit the well-behaved RGB space, represented as a cube in $[0,1]^3$. Therefore, I and R map to normalized RGB colors. First, let $G^{S_i} \in \mathbf{S}(S_i, 8)$ represent the set of 8 disjoint groups related to each of the cube's vertices, whose colors are $V = \{c_1, \ldots, c_8\}$, in which $c_i \in [0,1]^3$. RBD divides the RGB space according to the vertices of its cube representation and merges the white and black vertices to represent gray levels. Therefore, V corresponds to all possible combinations of RGB color channels. Let $x = \langle x_i \rangle_{i=1}^{m}$ a vector that indicates the color channels with maximum intensity in $I(p)$ such that $x_i = \mathbb{1}(I_i(p) = \|I(p)\|_\infty)$. We populate each $G_l^{S_i} \in G^{S_i}$ by assigning every $p \in S_i$ to its most similar group using a mapping function $M(p) = \operatorname{argmin}_{c_i \in V} \{\|x - c_i\|_1\}$.

Although $G_l^{S_i}$ contains pixels similar to c_l, they may present significantly distinct luminosities (*i.e.*, color shades), which can be suppressed if the mean color is desired. Thus, we split it into $\lambda \in \mathbb{N}^*$ subgroups (or *buckets*), denoted by $\widehat{G}_l^{S_i} \in \mathbf{S}(G_l^{S_i}, \lambda)$. Without abuse of notation, we insert every $p \in G_l^{S_i}$ into its respective group $\widehat{G}_{l,b}^{S_i}$ given $b = \lfloor \|I(p)\|_\infty \lambda \rfloor$. Therefore, each color group c_l is subdivided into λ buckets that correspond to the c_l color intensities.

We name *RGB Bucket Descriptor* (RBD) the descriptor $\text{RBD}(S_i) = \{c_1, ..., c_\alpha\}$, in which $c_i \in [0,1]^3$, resultant from the selection of the $\alpha \in \mathbb{N}^*$ most relevant colors within G^{S_i} by some predetermined criterion. In this work, $\text{RBD}(S_i)$ selects the average color $\mu(G_{l,b}^{S_i})$ of the most populated buckets, irrespective of l (*i.e.*, its vertex-based group). Although inaccurate for heterogeneous sets of pixels, the refinement for generating $G_{l,b}^{S_i}$ leads to a better approximation of the most predominant colors by the mean operator. On the other hand, by promoting such grouping, colors with visually indistinguishable differences are assigned to the same bucket, reducing the probability of selecting slight variations of the most frequent color.

B. Similarity between Image and Reconstruction from Superpixels

Given $\text{RBD}(S_i) = \{c_1, \ldots, c_\alpha\}$, one could generate a proper approximation of the original texture by the correct ordering, but such task is challenging. Conversely, we propose evaluating the best reconstruction possible from the most relevant colors for measuring the color variation description of S_i. Thus, we build $\mathcal{R}$ such that $R(p) = \operatorname{argmin}_{c_j \in \text{RBD}(S_i)} \{\|I(p) - c_j\|_1\}$.

After generating $\mathcal{R}$ from S, we may compute the *Mean Exponential Error* (MEE), shown in Equation 3 between it and the original image $\mathcal{I}$ for weighting each error accordingly:

$$\text{MEE}(S) = \frac{1}{|\mathbf{I}|} \sum_{S_i \in S} \sum_{p \in S_i} \|R(p) - I(p)\|_1^{2-\psi} \qquad (3)$$

in which $\psi = \max\{\|c_l - c_j\|_1\}$ and $c_l, c_j \in \text{RBD}(S_i)$. If a superpixel requires a palette of highly discrepant colors, the error impact should be greater since it is describing a complex pattern. Conversely, if the relevant colors are similar and, thus, are representing a more uniform texture, such impact must be light. Finally, we may define the *Similarity between Image and Reconstruction from Superpixels* (SIRS), in Equation 4, by a Gaussian distribution centered at MEE(S):

$$\text{SIRS}(S) = \exp^{-\frac{\text{MEE}(S_i)}{\sigma^2}} \qquad (4)$$

where σ^2 is a parameter that controls the importance we give to small error variations. In SIRS, higher the value, better is the color homogeneity of the superpixels in S, represented within $[0,1]$.

IV. Experimental Results

In this section, we describe the experimental setup for validating our proposal and discuss the impacts of the parameter selection (Section IV-A). Finally, in Sections IV-B and IV-C, we compare our proposal to the EV in quantitative and qualitative evaluations of five superpixel segmentation methods with varying segmentation qualities. Due to the IV not presenting normalized values and not being comparable with the EV and SIRS, we did not include the IV in the evaluation. The implementation of SIRS is available online at https://github.com/IsabelaBB/SIRS-superpixels.

We selected three different datasets which impose different challenges in assessing segmentation. *Birds* [12] consists of 150 images of Birds whose thin elongated legs are difficult to segment and, thus, may compromise the color description. *Sky* [13] has 60 images with large homogeneous regions with subtle luminosity variations. Finally, the *Extended Complex Scene Saliency Dataset* (ECSSD) [14] is composed of 1000 images with objects and backgrounds whose textures are complex. Moreover, we select five superpixel methods with different properties to evaluate SIRS' expressiveness, leading to distinct color variation descriptions. Specifically, DISF [15] and SH [16] are state-of-the-art methods in object delineation, while IBIS [17] and SLIC [18] present more compact superpixels with fair delineation. Finally, we consider a grid-based segmentation (GRID), representing a segmentation with maximum compactness but poor delineation.

A. Parameter Analysis and Suggestion

For evaluating the impact of RBD's α and λ in SIRS, we performed a grid-search for a varying $\alpha \in [1, 2, 4, 8]$ and $\lambda \in [8, 16, 32, 64]$ on a random selection of 30% of the Birds' images. From Figure 2, it is possible to infer that α and λ are highly correlated. By selecting $\alpha = 2$ and $\lambda = 32$, the reconstruction is compromised due to the reduced number of relevant colors selected in contrast to the low discretization of the color space (*i.e*, small color intervals are grouped on RBD). On the other hand, $\alpha = 8$ and $\lambda = 8$ offers a lighter penalization for few superpixels, which often present low-quality color variation description. Therefore, we opt for $\alpha = 4$ and $\lambda = 16$ since it severely penalizes for few superpixels, while selecting a fair quantity of relevant colors for reconstruction. Figure 3 illustrates the impacts on

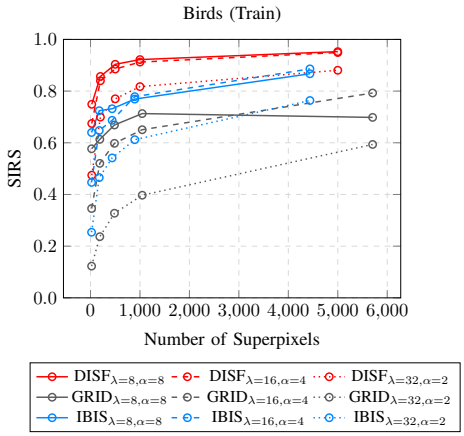

Fig. 2. Impact of different λ and α for varying superpixel numbers on the train images of Birds dataset with GRID (gray), IBIS (blue), and DISF (red) segmentations.

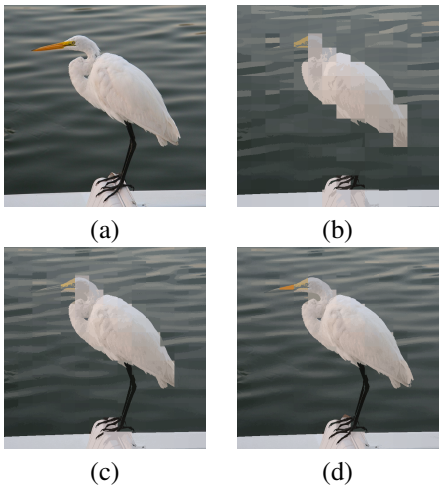

Fig. 3. Impact of different λ and α for image reconstruction using RBD. (a) Original Image; (b-d) Reconstructions using 200 superpixels using GRID with $\alpha \in \{2, 4, 8\}$ and $\lambda \in \{8, 16, 32\}$, respectively

such selection: by increasing α and λ, RBD is capable of improving the set of relevant colors, leading to a more accurate reconstruction. It is important to note that the reconstruction may have no errors for α values equal to the number of populated buckets. Therefore, the λ and α values are crucial for our proposal's performance.

Similarly, to evaluate the impact of the Gaussian variance σ^2, we evaluated varying it between $[0.005, 0.05]$ with step of 0.005. From Figure 4, we infer that σ^2 influences on the steepness of the curves, indicating lighter penalizations as σ^2 increases and, finally, reducing expressiveness. Therefore, for a fair error influence and a better spread of the curves, we opted for $\sigma^2 = 0.01$.

B. Quantitative Results

As one can see in Figure 5, both SIRS and EV distinguish methods which maximize delineation (*i.e.*, DISF and SH) with those opting for more compact superpixels (*i.e.*, GRID, SLIC, and IBIS). However, EV presents a lesser spread than

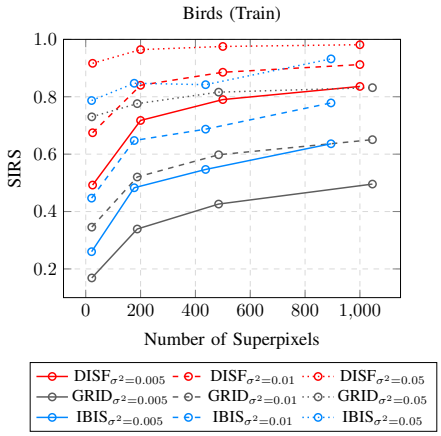

Fig. 4. Impact of different σ^2 for varying superpixel numbers on the train images of Birds dataset with GRID (gray), IBIS (blue), and DISF (red) segmentations.

SIRS, as exemplified in the distance between IBIS' and SH's curves. Moreover, EV tends to result in significantly higher values, especially in contexts where superpixels are increasingly heterogeneous. For example, GRID obtains a score over 0.5 on the Sky dataset with only 25 superpixels. Conversely, SIRS offers a more meticulous discrepancy even with methods with similar performance, like DISF and SH. Also, due to its penalization, SIRS exhibits a more coherent range of values when few superpixels are generated — *i.e.,* in a more heterogeneous segmentation. In the same example, GRID scored less than 0.4 on the same dataset.

C. Qualitative Results

Figure 6 presents a visual comparison between the evaluations obtained with SIRS and EV in segmentations of images with large homogeneous or texturized regions. As one may note in the Sky segmentations, EV is sensitive to color variations, leading to higher penalization in perceptually homogeneous regions — when, we argue, should be lighter. Moreover, seeing the ECSSD segmentation, EV often inaccurately scores the object superpixels as heterogeneous as those in the background. Finally, by increasing the superpixel quantity, EV shifts its perception of highly-variant superpixels mostly to those in the background, including homogeneous ones in the Sky segmentations. In contrast, SIRS consistently perceives homogeneous regions as low-variant ones, independently from the number of superpixels, in both Sky and ECSSD segmentations. We argue that such robustness is directly linked to the accurate selection of colors from RBD, properly describing superpixel homogeneity. Finally, it is worth noticing that, although SIRS may penalize more heterogeneous regions (*e.g.*, those with complex textures), it tends to be lighter than those from EV.

V. Conclusion

In this work, we propose a novel color homogeneity measure for superpixel segmentation assessment, named *Similarity between Image and Reconstruction from Superpixels* (SIRS).

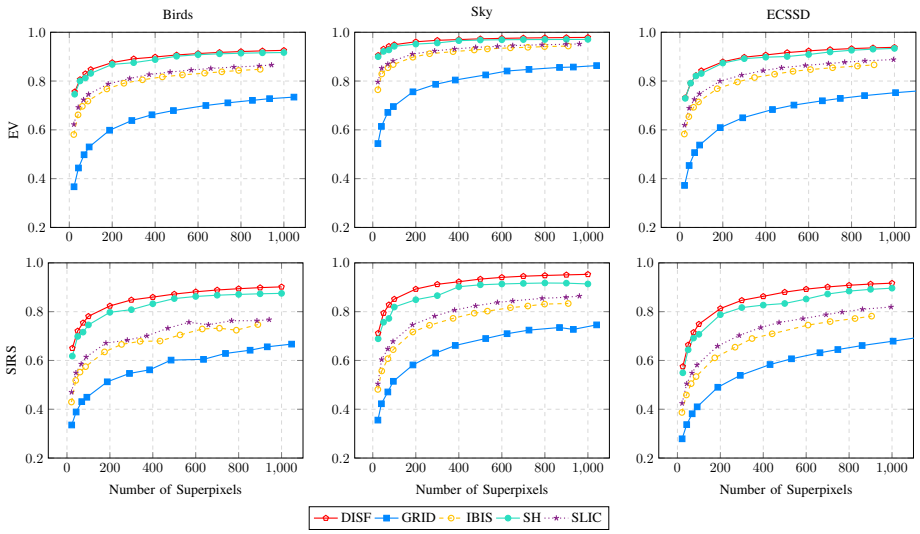

Fig. 5. Results obtained for Birds, Sky and ECSSD for EV and SIRS.

Our proposal evaluates a superpixel segmentation by its ability to reconstruct the original image from small sets with the most representative colors in each superpixel. Such selection is made using a new color descriptor named *RGB-cube Bucket Descriptor* (RBD), which collects the most representative colors per superpixel. Results show that RBD offers an accurate color selection, while SIRS presents expressiveness and robustness to color variations being able to better differentiate superpixel algorithms than the most popular measure of color homogeneity. For future work, we intend to explore the optimal selection for λ and α values and improve SIRS to highly correlate it with accurate object delineation.

Acknowledgment

The authors thank the Conselho Nacional de Desenvolvimento Científico e Tecnológico – CNPq – (Universal 407242/2021-0, PQ 303808/2018-7, 310075/2019-0), the Fundação de Amparo a Pesquisa do Estado de Minas Gerais – FAPEMIG – (PPM-00006-18), the Fundação de Amparo a Pesquisa do Estado de São Paulo – FAPESP – (2014/12236-1) and the Coordenação de Aperfeiçoamento de Pessoal de Nível Superior – CAPES – Finance code 001 (COFECUB 88887.191730/2018-00) for the financial support.

References

[1] Y. Liang, Y. Zhang, Y. Wu, S. Tu, and C. Liu, "Robust video object segmentation via propagating seams and matching superpixels," *IEEE Access*, vol. 8, pp. 53 766–53 776, 2020.

[2] W. Zhao, Y. Fu, X. Wei, and H. Wang, "An improved image semantic segmentation method based on superpixels and conditional random fields," *Applied Sciences*, vol. 8, no. 5, p. 837, 2018.

[3] L. Ren, L. Zhao, and Y. Wang, "A superpixel-based dual window rx for hyperspectral anomaly detection," *IEEE Geoscience and Remote Sensing Letters*, vol. 17, no. 7, pp. 1233–1237, 2019.

[4] X. Zhou, Y. Wang, Q. Zhu, C. Xiao, and X. Lu, "Ssg: superpixel segmentation and grabcut-based salient object segmentation," *The Visual Computer*, vol. 35, no. 3, pp. 385–398, 2019.

[5] P. Sellars, A. I. Aviles-Rivero, and C.-B. Schönlieb, "Superpixel contracted graph-based learning for hyperspectral image classification," *IEEE Transactions on Geoscience and Remote Sensing*, vol. 58, no. 6, pp. 4180–4193, 2020.

[6] D. Stutz, A. Hermans, and B. Leibe, "Superpixels: An evaluation of the state-of-the-art," *Computer Vision and Image Understanding*, vol. 166, pp. 1–27, 2018.

[7] D. R. Martin, C. C. Fowlkes, and J. Malik, "Learning to detect natural image boundaries using local brightness, color, and texture cues," *IEEE transactions on pattern analysis and machine intelligence*, vol. 26, no. 5, pp. 530–549, 2004.

[8] P. Neubert and P. Protzel, "Superpixel benchmark and comparison," in *Proc. Forum Bildverarbeitung*, vol. 6, 2012, pp. 1–12.

[9] W. Benesova and M. Kottman, "Fast superpixel segmentation using morphological processing," in *Conference on Machine Vision and Machine Learning*, 2014, pp. 67–1.

[10] A. P. Moore, S. J. Prince, J. Warrell, U. Mohammed, and G. Jones, "Superpixel lattices," in *2008 IEEE conference on computer vision and pattern recognition*. IEEE, 2008, pp. 1–8.

[11] R. Giraud, V.-T. Ta, and N. Papadakis, "Evaluation framework of superpixel methods with a global regularity measure," *Journal of Electronic Imaging*, vol. 26, no. 6, p. 061603, 2017.

[12] L. A. C. Mansilla and P. A. V. Miranda, "Oriented image foresting transform segmentation: Connectivity constraints with adjustable width," in *2016 29th SIBGRAPI Conference on Graphics, Patterns and Images (SIBGRAPI)*, 2016, pp. 289–296.

[13] E. B. Alexandre, A. S. Chowdhury, A. X. Falcao, and P. A. V. Miranda, "Ift-slic: A general framework for superpixel generation based on simple linear iterative clustering and image foresting transform," in *2015 28th SIBGRAPI Conference on Graphics, Patterns and Images*, 2015, pp. 337–344.

[14] J. Shi, Q. Yan, L. Xu, and J. Jia, "Hierarchical image saliency detection on extended cssd," *IEEE transactions on pattern analysis and machine intelligence*, vol. 38, no. 4, pp. 717–729, 2015.

[15] F. C. Belém, S. J. F. Guimarães, and A. X. Falcão, "Superpixel segmentation using dynamic and iterative spanning forest," *IEEE Signal Processing Letters*, vol. 27, pp. 1440–1444, 2020.

[16] X. Wei, Q. Yang, Y. Gong, N. Ahuja, and M.-H. Yang, "Superpixel hierarchy," *IEEE Transactions on Image Processing*, vol. 27, no. 10, pp. 4838–4849, 2018.

[17] S. Bobbia, R. Macwan, Y. Benezeth, K. Nakamura, R. Gomez, and J. Dubois, "Iterative boundaries implicit identification for superpixels segmentation: a real-time approach," *IEEE Access*, vol. 9, pp. 77 250–77 263, 2021.

[18] R. Achanta, A. Shaji, K. Smith, A. Lucchi, P. Fua, and S. Süsstrunk, "Slic superpixels compared to state-of-the-art superpixel methods," *IEEE Transactions on Pattern Analysis and Machine Intelligence*, vol. 34, no. 11, pp. 2274–2282, 2012.

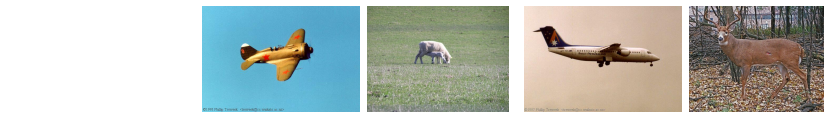

(a) Original images

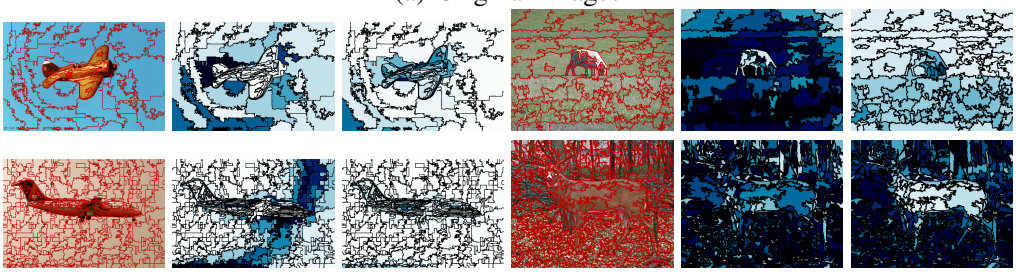

(a) DISF

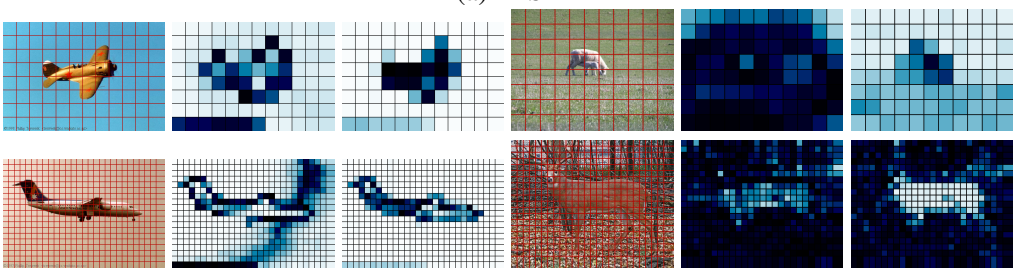

(b) GRID

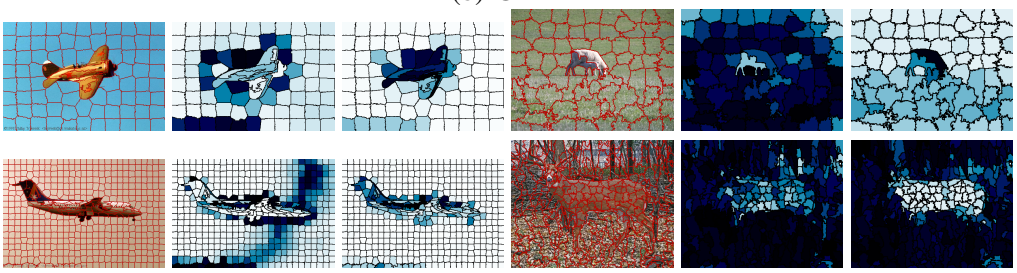

(c) IBIS

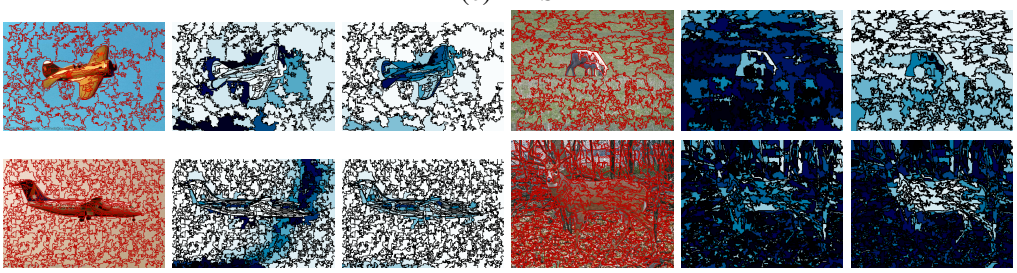

(d) SH

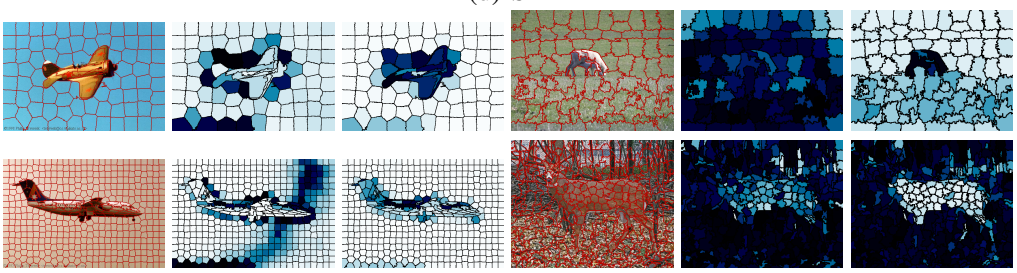

(e) SLIC

Fig. 6. Segmentation comparison with (a) images from Sky and ECSSD among (b) DISF, (c) GRID, (d) IBIS, (e) SH, and (f) SLIC. In (b)-(f), segmentations in first and fourth columns have 100 and 500 superpixels, respectively. The second and fifth column in (b)-(f) present the EV evaluation representation (whiter values indicate higher scores), and it is analogous for the third and sixth columns for SIRS.